Recent Developments in Bridge Engineering

Edited by Khaled M. Mahmoud

Recent Developments in Bridge Engineering, Mahmoud (ed.)
© 2003 Swets & Zeitlinger, Lisse, ISBN 90 5809 606 8

Transient response simulation of a composite material footbridge to crossing pedestrians

P.J. Fanning & P. Archbold
Department of Civil Engineering, University College Dublin, Ireland

A. Pavic & P. Reynolds
Department of Civil and Structural Engineering, University of Sheffield, UK

ABSTRACT: Loads applied by pedestrians, and crowds of pedestrians, are particularly important for footbridges with natural frequencies close to footfall frequencies of moving pedestrians. Recorded response data from Aberfeldy Bridge, an advanced composite material footbridge in Scotland, for numerous pedestrian crossings reveals both vertical and lateral response components. No provision is made in existing codes of practice for the calculations of actual dynamic responses of pedestrian footbridges to lateral pedestrian-induced load. The authors are seeking to develop an appropriate pacing frequency-dependent lateral load model, to be used in conjunction with existing vertical load models that would account for such lateral excitation. This is done by correlation of the measured bridge dynamic response with the results of the simulations where a validated numerical model has been utilised. The modelling techniques used to correlate the modal properties of the finite element model with the real structure are described in this paper. Subsequently the modelling and transient solution strategies used to simulate the vertical footbridge response at different pacing frequencies are compared to actual bridge measurements to good effect. Finally a structure for the form of the lateral load model required to capture pacing frequency dependent lateral effects is also proposed.

1 INTRODUCTION

Research in the area of human-structure dynamic interaction has been catalyzed in recent years following the opening of the Millennium Footbridge in London during 2000 and its subsequent excessive response to pedestrian loading.

A comprehensive study of the bridge response, induced by crowds of people crossing the bridge, revealed a significant horizontal load component that was previously not recognized or understood by the engineering profession, (Dallard et al, 2001). This horizontal load component was attributed to synchronous lateral excitation, which describes the manner in which pedestrians walk in phase with lateral bridge vibration, once this vibration reaches a perceptible level, and thereby impose an additional lateral load, which is in phase with the bridge response.

This lateral load is particularly important for those footbridges with lower lateral frequencies close to footfall frequencies of moving pedestrians. Aberfeldy footbridge in Scotland is one of the first bridges in the world to be made almost entirely of advanced composite materials; additionally its lowest mode of vibration is a lateral one with a frequency close to the footfall frequency of a normal pacing rate. In-situ tests undertaken by a team from the University of Sheffield demonstrated that levels of vertical and lateral excitations were functions of pacing frequency.

The transient response of Aberfeldy Bridge to crossing pedestrians is discussed in this paper. Initially the construction of a validated numerical model, capable of capturing the fundamental modal characteristics of the bridge, is discussed. Subsequently the vertical response of the bridge to crossing pedestrians is simulated to examine the suitability of existing vertical load models in predicting the bridge response. Finally a structure for the form of a lateral load model is proposed. Enhancements for both vertical and lateral load models are also discussed.

2 ABERFELDY FOOTBRIDGE

Aberfeldy footbridge (Figure 1) is a cable-stayed footbridge over the River Tay at the Aberfeldy Golf Course in Aberfeldy, Scotland. Its main span is 63 m long and it has two side spans of 25 m each. It is constructed almost entirely from a Glass-Fibre Reinforced Polymer (GRP) composite material. The basic components of construction are a plank 600 mm wide by 80 mm thick, with 3 mm walls forming seven cells and a three-way connector piece, which provides the ability to connect sections side by side or in T formations. A dog-bone toggle fits into grooves running longitudinally along the sides of these components to connect them together.

The bridge deck (Figure 2) is three planks and two connectors wide. The handrails are supported one cell in from the edge of the deck. The edge of the plank is stiffened with an edge beam constructed from four, five or six connectors arranged in a vertical column or an L shape. The cables are attached to cross beams made up from four connectors. Single connectors, acting as crossbeams at approximately 1 m centres between the cable supports, complete the framing of the deck. Over the main span, some of the cells in the planks were filled with a ballast material to prevent uplift in high winds and to separate the torsion and vertical modes of vibration.

The tower section is constructed from 4 planks and four connectors forming an enclosed square section and they each support 20 cables. Each of the cables has a Kevlar 49 core in a polythene sheath. The four upper cables at each tower are 20 mm diameter, while the remaining cables are 17 mm diameter. Along the side-spans, aluminium ties tie the cables and deck back to the foundations.

Some remedial work was performed in 1997 in which additional GRP slats were bonded and riveted to the surface of the deck.

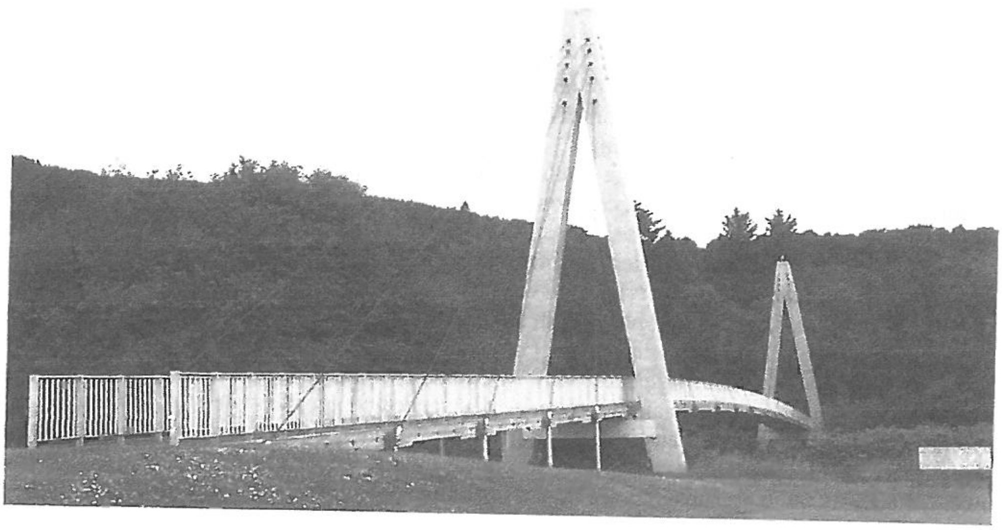

Figure 1. Aberfeldy footbridge.

3 FINITE ELEMENT MODELLING

3.1 *Geometry of finite element model*

The bridge was modelled in ANSYS v5.7 and has 5 main structural components: the deck, the crossbeams, the towers, the cables and the aluminium ties.

The planks in the deck were modelled using 4 noded shell elements (SHELL181). These elements were assigned a thickness of 3 mm along the top and bottom surfaces and all the inner surfaces. Where the plank joined a connector (i.e. where there were two surfaces adjacent to each other) the shell elements were assigned a thickness of 6 mm.

The crossbeams were modelled using linear beam elements and modelled along the bottom line of the deck elements. A cross-section of the FE representation of the deck is shown in Figure 3.

The distribution of additional masses such as deck finishing, ballast in some cells of the central plank, handrails and the additional slats was modelled accurately by assigning additional masses appropriately to the various shell elements.

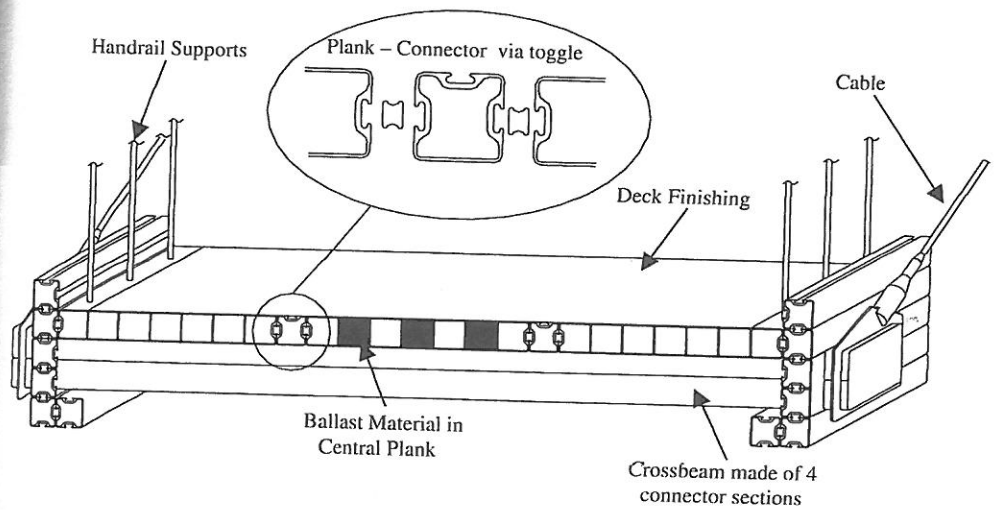

Figure 2. Cross-section of GRP plank and 3-way connector.

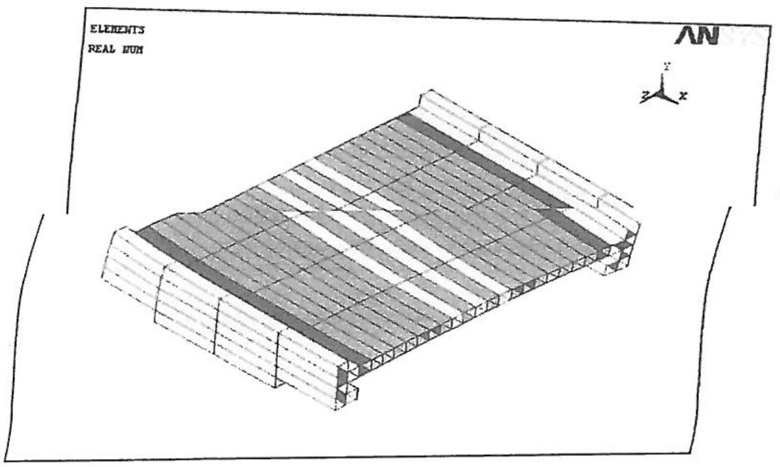

Deck representation in FE model

The towers were also modelled using linear beam elements. The two legs of the towers are joined at the top cable anchorage positions by beams of the same material, but with zero mass.

The cables were modelled using spar elements and were connected to the crossbeams in the deck. The aluminium ties in the side spans were also modelled using spar elements. The 3D FE model is shown in Figure 4.

3.2 *Material properties*

The GRP material was modelled using an orthotropic material model with material constants as specified by Maunsells Ltd., the manufacturers of the bridge components. Manufacturers data sheet values were used for the cable properties. Standard established values were used for the aluminium ties. The material properties used, in an initial model, are listed in Table 1.

3.3 *Boundary conditions*

The two towers were fully fixed at their bases, as were all of the aluminium ties in the side spans. The ends of the deck are restrained against translation in all directions at one end and in the vertical and transverse directions only at the other.

3.4 *Modal analysis procedure*

The extraction of natural frequencies and mode shapes required two sequential analysis steps. An initial static analysis of the bridge, under its own self-weight, was invoked to simulate the in-situ

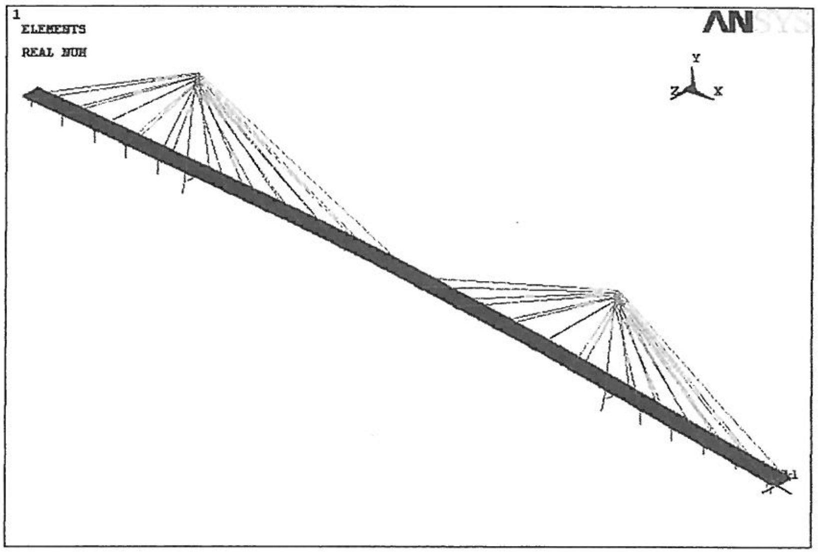

Figure 4. Isometric view of entire FE model.

Table 1. Material properties used in initial FE model.

	Symbol	Unit	GRP	Kevlar	Aluminium
Longitudinal modulus	E_x	GPa	24.7	126.5	70
Transverse modulus	E_y	GPa	8.13	n/a	n/a
Poisson's ratio	n_{xy}	–	0.08	0.3	0.3
Poisson's ratio	n_{yx}	–	0.27	n/a	n/a
Shear modulus	G_{xy}	GPa	3.9	n/a	n/a
Density	r	kg/m^3	1750	2618	2700

stresses in the cables and the deck. A subsequent eigenvalue analysis was run on the stressed structure to determine the first 20 natural frequencies and modes of vibration of the bridge.

3.5 *Results from original FE model*

The predicted modes of vibration and associated natural frequencies from the original FE model along with those measured by Pavic et al (2000) are tabulated in Table 2. Vi represents the ith vertical mode shape, Lj represents the jth lateral mode shape and Tk represents the kth torsional mode shape. The figures in parentheses represent the percentage differences between the predicted and measured natural frequencies.

In the first analysis, (Set 1), using material properties as in Table 1, the fundamental frequency of the first lateral mode was 16% higher than the measured value, with the frequency of the second lateral mode being 11% higher than the measured value. The frequency of the first 6 vertical modes was within 7% of the measured values.

Considering that the mass was modelled fairly accurately (compared to the stiffness), the higher analytical frequencies indicate that the FE model overestimated the stiffness of the bridge, although the sequence of vertical and lateral modes is consistent with the measured data. It is interesting to note that the numerical predictions of the frequencies of the torsional modes of vibration also demonstrated an overestimation of the torsional stiffness in the FE model.

3.6 *Updating of FE model*

Following this initial analysis a series of sensitivity studies was undertaken, Table 3. The lateral modes were found to be most sensitive to the Young's Modulus of the GRP in the span direction, while the vertical modes were found to be most sensitive to the stiffness of the cables. Other parameters such as the transverse Young's Modulus of the GRP and the Young's Modulus of the aluminium struts were found to have negligible effect on the natural frequencies of any of the modes. As the mass of the bridge determined in the static analysis closely matched the reported total mass of the bridge (Pavic et al, 2000), neither the density of the materials nor the additional masses applied were varied.

Following these sensitivity studies, and mindful of the fact that the material properties specified in the model were standard manufacturer's data and not site specific, the model was manually updated to match the measured natural frequencies.

For a longitudinal Young's Modulus of the GRP of 80% of its original value natural frequencies for the first three lateral modes were predicted to within 7% of the measured values, while the first 8 vertical modes were all within 6%. The values for the first three torsional modes were improved by approximately 2%.

Table 2. Comparison of measured and calculated mode shapes and natural frequencies.

Mode shape number	Measured frequency (Hz)	Calculated frequency (from original FE model) (Hz)
L1	0.98	1.14 (+16%)
V1	1.52	1.63 (+7%)
V2	1.86	1.94 (+4%)
V3	2.49	2.62 (+5%)
L2	2.73	3.04 (+11%)
V4	3.01	3.11 (+3%)
V5	3.50	3.63 (+4%)
V6	3.91	4.00 (+2%)
T1	3.48	4.17 (20%)
V7	4.40	4.45 (+1%)
V8	4.93	4.90 (−1%)

Table 3. Comparison of measured and calculated mode shapes and natural frequencies.

Mode shape number	Measured frequency (Hz)	Calculated frequency (Hz) Initial values (Set 1)	Ex of GRP at 80% & E of Kevlar at 90% (Set 2)	Ex of GRP at 80% & E of Kevlar at 90% spring stiffness 5 × 10^6 N/mm^2 (Set 3)
L1	0.98	1.14 (+16%)	1.04 (+6%)	1.018 (+3.8%)
V1	1.52	1.63 (+7%)	1.54 (+1%)	1.537 (+1.1%)
V2	1.86	1.94 (+4%)	1.82 (−2%)	1.822 (−2.0%)
V3	2.49	2.62 (+5%)	2.45 (−2%)	2.458 (−1.3%)
L2	2.73	3.04 (+11%)	2.78 (+2%)	2.720 (−0.3%)
V4	3.01	3.11 (+3%)	2.89 (−4%)	2.902 (−3.6%)
V5	3.50	3.63 (+4%)	3.38 (−3%)	3.382 (−3.4%)
V6	3.91	4.00 (+2%)	3.71 (−5%)	3.715 (−5.0%)
T1	3.48	4.17 (20%)	3.94 (+13%)	3.943 (+13.3%)
V7	4.40	4.45 (+1%)	4.12 (−6%)	4.124 (−6.27%)
V8	4.93	4.90 (−1%)	4.52 (−8%)	4.519 (−8.3%)

Reducing the cable stiffness to 90% of their original value there was little change in the values of the lateral frequencies, while the predicted natural frequencies of the first 8 vertical modes were all within 3% of the measured values. The values for the first three torsional modes were improved by up to 8%.

A combination of the cable stiffness at 90% of its original value and the longitudinal modulus of the GRP at 80% of its original value (Table 3, Set 2) brought predictions of the frequencies for the lateral modes to within 7% of the measured values and predictions for the vertical modes to within 8% of the measured values. The values for the torsional modes were also closer to the measured values.

Improved correlation was further achieved by adjusting the stiffness of the bearings between the pylons and the deck (Table 3, Set 3). A bearing stiffness 5 × 10^6 N/m was specified in the final model. In addition to varying the bearing stiffness in the vertical direction, spring elements in the transverse direction were also considered and their stiffness varied. It was found that lateral bearing stiffness was best modelled using infinitely stiff elements.

3.7 *Determination of damping coefficients for aberfeldy footbridge*

Following experimental modal testing of the bridge, damping values were determined for each of the measured natural frequencies. In performing a transient analysis in ANSYS the damping matrix is considered to be proportional to either, or both, of the mass and stiffness matrices;

$$[C] = \alpha[M] + \beta[K]$$

where [M] and [K] are the global mass and stiffness matrices and α and β are constants. The percentage of critical damping, ξ_j, simulated at any natural frequency, ω_j, modelled in this way is given by:

$$\xi_i = 0.5 \left([\alpha \div \omega_j] + [\beta \, \omega_j] \right)$$

The experimental modal damping ratios for the vertical and lateral modes are plotted against natural frequencies in Figure 5. The increase in damping levels with natural frequency is consistent with stiffness proportional damping. Mass proportional damping was not considered ($\alpha = 0$) and regression analysis of the values plotted in Figure 5 was used to calculate a β value, which was subsequently used in the transient response simulations.

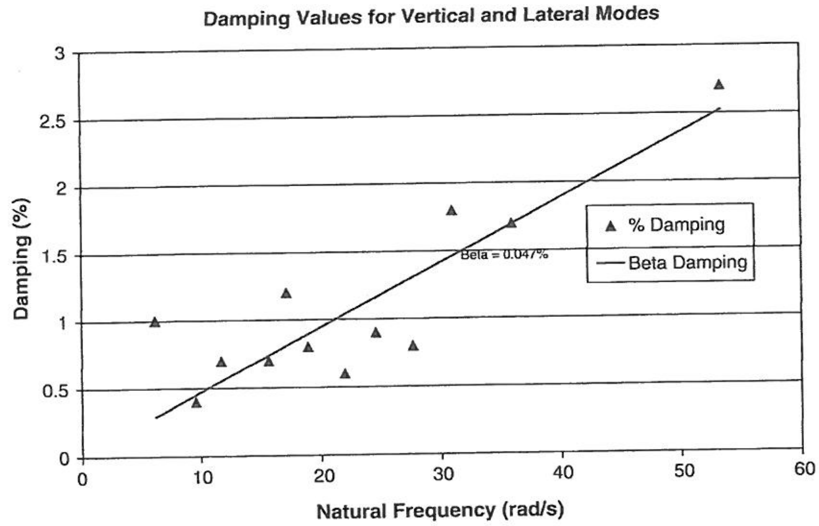

Figure 5. Calculation of damping coefficients.

Table 4. Test subjects & pacing frequencies simulated.

Test subject	Mass (kg)	Height (m)	Pacing frequency simulated (Hz) (V) = vertical (L) = lateral (V + L) = both
TS1	104	1.90	1.4(V) 1.5(V) 1.6(V + L) 1.7(V + L) 1.8(V + L) 1.9(V + L) 2.0(V + L)
TS5	86	1.93	1.4(V) 1.5(V) 1.6(V) 1.7(V + L) 1.8(V + L) 1.9(V + L) 2.0(V + L)

4 TESTING ON ABERFELDY FOOTBRIDGE

Pavic et al (2000) recorded vibration measurements from Aberfeldy footbridge for 100 crossings of the bridge by 8 different test subjects. A total of 59 controlled measurements were made with pacing rates varying from 1.4 Hz to 2.0 Hz in increments of 0.1 Hz. The controlled tests involved the test subjects walking at a specific rate, controlled by use of a metronome. The "not controlled" tests were done without the use of a metronome and involved the subjects walking at nominal pacing frequencies. Test subjects TS1 and TS5 both partook in the controlled tests – their masses and the pacing rates at which they crossed the bridge are summarized in Table 4.

5 VERTICAL FORCE SIMULATION

The vertical load model used in existing codes of practice for the design of pedestrian footbridges is based on the assumption that loading from walking is cyclic in nature. The vertical force exerted consists of a static load plus a time-varying dynamic component, which is represented by a combination of Fourier terms. The load model is based on the work of Bachmann (1987) who reported that the time dependent vertical load from a walking pedestrian could be reasonably simulated using only the first three harmonics of the pacing frequency:

$$F(t) = G + \Delta G_1 \sin(2\pi f_s t) + \Delta G_2 \sin(4\pi f_s t - \phi_2) + \Delta G_3 \sin(6\pi f_s t - \phi_3) \quad (1)$$

where:

G = static force from pedestrian (Mass × 9.81 m/s^2)
ΔG_n = $r_n G$ = load component of nth harmonic
f_s = pacing frequency
t = time
ϕ_n = phase angle between harmonics

Bachmann (1987) proposes further that the value for r_1, the vertical load factor for the first harmonic, is 0.4 for $f_s = 2.0$ Hz and 0.5 for $f_s = 2.4$ Hz with linear interpolation between these values.

The moving test subjects were modelled as a series of time dependent loads moving along the bridge deck. Assuming a stride length of 0.9 m, and knowing the pacing rate for different tests, the velocity of the test subject was determined from which the appropriate load position was derived. The magnitude of the applied load was subsequently determined using Equation (1).

5.1 *Effect of higher order harmonics on load simulation*

Figure 6(a) shows the 2s rms traces respectively from simulations of vertical loading from TS1 walking at a pacing rate of 1.8 Hz and comparisons with test data. Simulations for a single harmonic and three harmonics of loading are compared to measured data. For the single harmonic simulation a load factor of 0.35, determined by extrapolation outside the range proposed by Bachmann (1987) above, was specified for the first harmonic. In the case of three harmonics a load factor of 0.35 was applied for the first harmonic with factors 0.1 for both the second and third harmonics based on work by Schulze (1980) and Baumann & Bachmann (1987)

The simulation of the loading applied considering only the first harmonic gives the more accurate representation of the measured response. Furthermore a Fast Fourier Transform analysis performed on the two measured passes, Figure 6(b), indicates that there is little evidence of significant input from higher harmonics of the pacing rate (no peaks). The single harmonic simulation is consistent with the bridge response while the simulation using three harmonics shows a significant contribution from the higher harmonics. In subsequent simulations for TS1 and TS5, at different pacing rates, only the first harmonic of loading was considered.

5.2 *Load factor associated with first harmonic of pacing frequency*

Equation 2 illustrates the mathematical relationship between pacing frequency and first harmonic load factor as reported by Bachmann (1987) for frequencies between 2.0 and 2.4 Hz.

$$r_n = 0.25 f_s - 0.1 \qquad (2)$$

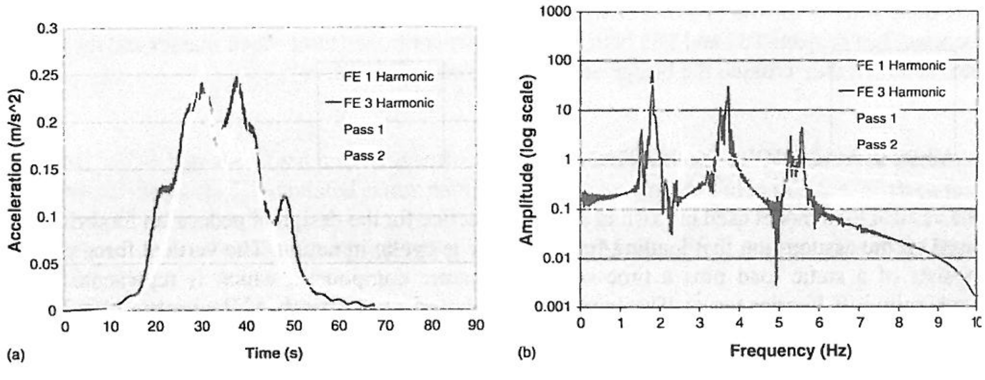

Figure 6. (a) 2s rms of TS1 at a pacing rate of 1.8 Hz, (b) FFT of measured and predicted responses of Aberfeldy footbridge to TS1 crossing at a pacing rate of 1.8 Hz.

The first pacing rate simulated was 1.8 Hz for both TS1 and TS5, using the following formula:

$$F(t) = G + \Delta G_1 \sin(2\pi f_s t) = G + r_1 G \sin(2\pi f_s t) \quad (3)$$

Using Equation 2 and extrapolating for a pacing rate of 1.8 Hz gives a load factor for the first harmonic of 0.35. Figure 7(a) shows the results for the 2s rms acceleration traces for TS1 walking at 1.8 Hz, while Figure 8(a) shows the 2s rms traces for TS5 walking at 1.8 Hz. Figure 7(b) and Figure 8(b) show the corresponding 10s rms traces. The measured responses, for the two passes of each test subject at a 1.8 Hz pacing frequency, are also included for comparison. In subsequent simulations at different pacing frequencies Equation 2 was also used to determine the load factor for the first harmonic of loading.

5.3 *Results of vertical simulations*

Maximum predicted and measured vertical accelerations, at midspan, for TS1 and TS5 at a pacing rate of 1.8 Hz are given in Table 5. Maximum root mean squared (rms) accelerations for 2-second and 10-second intervals are also compared. Pass 1 refers to a South – North crossing while Pass 2 is the return crossing. In general there is good agreement between the numerical model and the measured data. The 10s rms values are within 3% of each other, while the 2s rms traces show less than 11% difference between the predicted and measured values.

Predicted and measured RMS accelerations for TS1 and TS5 at different pacing rates are compared in Tables 6 and 7 along with the various first harmonic load factors, based on Equation 2, used in each simulation. The results of the 10s rms traces yielded maximum values as shown in Table 6, while

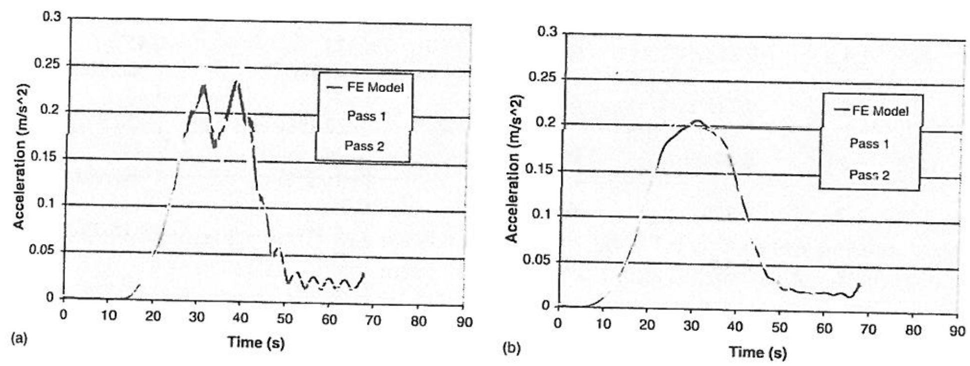

Figure 7. (a) 2s rms from TS1 at 1.8 Hz, load factor = 0.35, (b) 10s rms from TS1 at 1.8 Hz, load factor = 0.35.

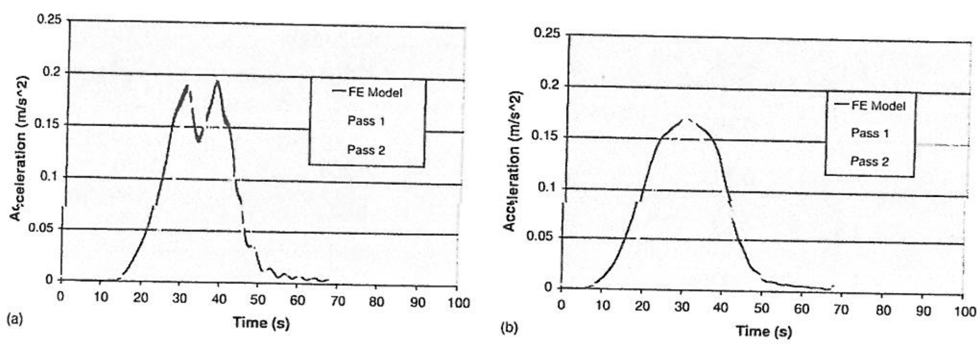

Figure 8. (a) 2s rms from TS5 at 1.8 Hz load factor = 0.35, (b) 10s rms from TS5 at 1.8 Hz load factor = 0.35.

Table 5. Results from simulations of TS1 & TS5 at 1.8 Hz.

Test Subject	Test Number	Max. acceleration (m/s^2)	Max. 2s rms acceleration (m/s^2)	Max. 10s rms acceleration (m/s^2)
TS1	Pass 1	0.397	0.265	0.215
	Pass 2	0.393	0.262	0.205
	Average of Pass 1 & 2	0.395	0.264	0.210
	FE model	0.336	0.235	0.206
	% Error of FE results*	−14.9%	−10.9%	−1.9%
TS5	Pass 1	0.282	0.193	0.172
	Pass 2	0.284	0.181	0.162
	Average of pass 1 & 2	0.283	0.187	0.167
	FE model	0.277	0.195	0.171
	% Error of FE results*	−2.1%	+4.2	+2.3%

* Error measured as percentage difference between the calculated FE values and the average of the measured values.

Table 6. Peak 10s rms values for different pacing rates: vertical vibration.

Test subject	Pacing rate (Hz)	1st harmonic load factor	Simulated values (m/s^2)	Pass 1 measured values (m/s^2)	Pass 2 measured values (m/s^2)
TS1	1.4	0.25	0.349	0.334 (+4.5%)	0.457 (+26.9%)
	1.5	0.275	0.865	1.13 (−22.1%)	1.15 (−24.8%)
	1.6	0.30	0.615	0.558 (+10.2%)	0.449 (+36.9%)
	1.7	0.325	0.284	0.288 (−1.4%)	0.335 (−15.2%)
	1.8	0.35	0.206	0.215 (−4.2%)	0.205 (+0.4%)
	1.9	0.375	0.170	0.162 (+4.9%)	0.150 (+13.3%)
	2.0	0.40	0.176	0.161 (+9.3%)	0.153 (+15.0%)
TS5	1.4	0.25	0.289	0.266 (+8.6%)	0.214 (+35.0%)
	1.5	0.275	0.978	0.515 (+89.9%)	0.694 (+40.9%)
	1.6	0.30	0.509	0.275 (+85.1%)	0.269 (+89.2%)
	1.7	0.325	0.235	0.200 (+17.5%)	0.201 (+16.9%)
	1.8	0.35	0.171	0.172 (−0.6%)	0.162 (+5.5%)
	1.9	0.375	0.140	0.136 (+2.9%)	0.150 (−6.7%)
	2.0	0.40	0.145	0.132 (+9.8%)	0.136 (+6.6%)

Prior research in this area and the recorded data from Aberfeldy footbridge suggest that consideration should be given to lateral load models that include a velocity dependent term also.

ACKNOWLEDGEMENTS

The authors would like to acknowledge Arup Consulting Engineers for their permission to use the Aberfeldy bridge response data in this study.

REFERENCES

Bachmann, H. & Ammann, 1987. Vibrations in Structures Induced By Man and Machines, International Association for Bridge and Structural Engineering, *Structural Engineering Document*, Zurich, 1987.

Baumann, K. & Bachmann, H. 1987. Dynamic Loading Induced by Persons and Its Effect on Beam Structures, *Institute of Structural Engineering, Swiss Fed. Inst. of Tech (ETH), Zurich, report 7501–3 Birkhauser, Basle.*

Dallard, P., Fitzpatrick, T., Flint, A., Lowe, A. & Ridsill Smith, R. 2001. The Millennium Bridge, London: Problems & Solutions. *The Structural Engineer, Vol. 79, No. 8, pp. 15-17.*

Ellis B.R. & Ji, T. 1994. Floor Vibration Induced by Dance Type Loads: Verification *The Structural Engineer, Vol. 72, No. 3, pp. 45–50.*

Pavic, A., Reynolds, P., Cooper, P. & Harvey, W.J. (2000) Dynamic Testing and Analysis of Aberfeldy Footbridge, *Report by Department of Civil & Structural Engineering, Vibration Engineering Research Section, The University of Sheffield, Sir Frederick Mappin Building, Mappin Street, Sheffield S1 3JD, United Kingdom.*

Schulze, H. 1980. Dynamic Effects of the Live Load on Footbridges, *Signal und Schiene, Vol. 24, No. 2 pp. 91–93 and No. 3 pp. 143–147.*

Young, P. (2001) Improved Floor Vibration Prediction Methodologies, *Proceedings Arup's Seminar on Structural Vibration and Structure-borne Noise: Current Developments in Assessment and Design, 4 October 2001, IMechE London.*

The Bridge Engineering Association organized the 2nd New York City Bridge Conference with a distinguished group of renowned bridge engineers from all over the world.

On October 20-21, 2003, bridge engineers from different walks of the industry presented papers that are of considerable value to the bridge engineering profession.

This book contains a selected number of papers that were presented at the conference. These papers will enhance the practical application for any reader in the field of bridge engineering.

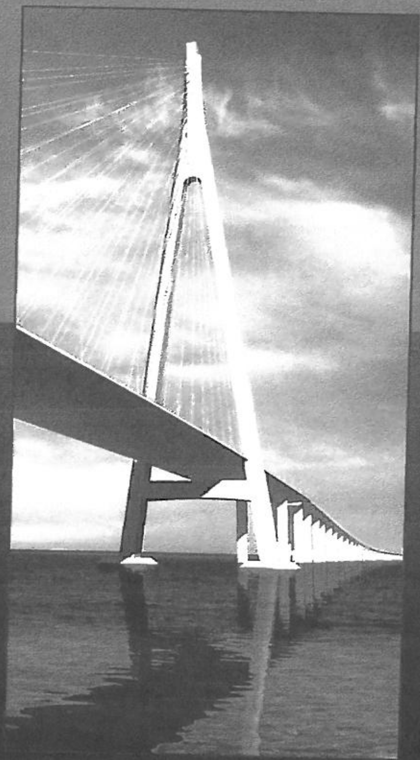

Bridge engineering technology has made tremendous advances covering a wide range of issues in the past few years. These include bridge design, new materials, rehabilitation of existing bridges, and building new bridges with record-setting span lengths and innovative construction techniques. The constant increase in traffic loads, associated with the substantial economic growth in modern societies imparts large demands on bridge structures. This, in part, contributes to the decaying condition of many bridges, an issue that has become a major concern to the international bridge engineering community. It is therefore of paramount importance that bridge engineers from different countries exchange knowledge, information and experience concerning the common challenges that confront our industry. It is such a global framework that distinguishes the 2nd New York City Bridge Conference with the presentation of state-of-the-art papers from different countries on a wide spectrum of topics in bridge engineering.

The conference was notable for its international impact. Experts presented papers from Austria, Canada, England, France, Germany, Ireland, Italy, Japan and Norway. These, along with contributions from an impressive list of U.S. experts, assure the lasting value of this volume.